

# UNCLASSIFIED

AD NUMBER
AD406875
NEW LIMITATION CHANGE
TO Approved for public release, distribution unlimited
FROM Distribution authorized to U.S. Gov't. agencies only; Administrative/Operational Use; FEB 1963. Other requests shall be referred to Army Research and Development Lab., Fort Belvoir, VA 22060.
AUTHORITY
USAERDL Itr, 17 Nov 1965

THIS PAGE IS UNCLASSIFIED

**UNCLASSIFIED**

**AD 406 875L**

**DEFENSE DOCUMENTATION CENTER**

**FOR**

**SCIENTIFIC AND TECHNICAL INFORMATION**

**CAMERON STATION, ALEXANDRIA, VIRGINIA**



**UNCLASSIFIED**

**NOTICE:** When government or other drawings, specifications or other data are used for any purpose other than in connection with a definitely related government procurement operation, the U. S. Government thereby incurs no responsibility, nor any obligation whatsoever; and the fact that the Government may have formulated, furnished, or in any way supplied the said drawings, specifications, or other data is not to be regarded by implication or otherwise as in any manner licensing the holder or any other person or corporation, or conveying any rights or permission to manufacture, use or sell any patented invention that may in any way be related thereto.

CATALOGED BY DDC

AS AD NO. 406875

LAS-SR-224-12  
February 1963

## ANGULAR ENERGY DISTRIBUTION OF PHOTOELECTRONS

Quarterly Progress Report  
16 October 1962 to 16 January 1963  
(Third Quarter)

Contract No. DA-44-009-ENG-5004

Prepared for

Warfare Vision Branch  
U. S. Army Research and Development Laboratories  
Ft. Belvoir, Virginia

THE UNIVERSITY OF CHICAGO  
LABORATORIES FOR APPLIED SCIENCES  
CHICAGO 37, ILLINOIS

NO OTS

LAS-SR-224-12  
February 1963

THE VIEWS CONTAINED HEREIN REPRESENT  
ONLY THE VIEWS OF THE PREPARING AGENCY  
AND HAVE NOT BEEN APPROVED BY THE  
DEPARTMENT OF THE ARMY.

## ANGULAR ENERGY DISTRIBUTION OF PHOTOELECTRONS

Quarterly Progress Report  
16 October 1962 to 16 January 1963  
(Third Quarter)

Contract No. DA-44-009-ENG-5004

Prepared for

Warfare Vision Branch  
U. S. Army Research and Development Laboratories  
Ft. Belvoir, Virginia

THE UNIVERSITY OF CHICAGO  
LABORATORIES FOR APPLIED SCIENCES  
CHICAGO 37, ILLINOIS

### ASTIA AVAILABILITY NOTICE

U. S. Government agencies may obtain copies  
of this report directly from ASTIA. Other  
qualified ASTIA users should request thru  
Director, USAERDL, Fort Belvoir, Virginia.

## FOREWORD

This report was prepared by the Laboratories for Applied Sciences of The University of Chicago under United States Army Research and Development Laboratories Contract No. DA-44-009-ENG-5004, "Angular Energy Distribution of Photoelectrons," LAS Task 27, registered for USAERDL by Mr. Edward J. Walker. It covers the quarter of the contract from 16 October 1962 to 16 January 1963.

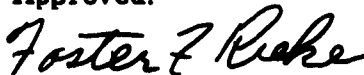
Laboratories for Applied Sciences personnel participated in the work covered in this report include R. Allison, J. E. F. Gillespie, E. Pekol, R. Pernic, and M. Remdt.

### LABORATORIES FOR APPLIED SCIENCES



Jay Burns  
Principal Investigator

Approved:



Foster F. Rieke  
Associate Director

## ABSTRACT

Initial test results on the experimental tube and associated apparatus are described together with certain changes suggested by the test results. Problems connected with making S-9 photocathodes by the atomic beam cesiation method have delayed angular distribution measurements. A tube is described which was built for experiments to correlate photoelectric properties with impurity concentrations in photocathodes as determined by Hall effect measurements. Certain theoretical aspects of the angular energy distribution are discussed.

## 1. EXPERIMENTAL

Experimental work during the reporting period centered on testing the complete experimental apparatus and especially the tube in which measurements are made. Several changes in tube components were made as a result of the tests. These will be described below.

A second experimental tube was built to measure the excess carrier concentration in photocathodes by the Hall effect and to measure yield, spectral sensitivity, and energy distribution of photoelectrons (integrated over all emission angles) in the same photosurfaces. The objective here is to study the relation of these photoelectric characteristics to the excess carrier concentration with emphasis upon the relative contributions of the surface and volume photoeffects in  $\text{Cs}_3\text{Sb}$ . It is important to have some information about the relative importance of surface and volume effects before the energy angular distribution can be treated theoretically. This point will be discussed more fully in the theory section.

### 1.1 Vacuum Processing and Components

Helium leak testing revealed small leaks in a large inconel bellows that transmits motion into the angular distribution tube to rotate the photocathode (see 1st Quarterly Report, LAS-SR-224-4). These leaks either developed in a heliarc weld that was inaccessible for repairs once the tube was assembled, or they were due to a porous section of the bellows that developed during vacuum firing prior to assembly. In any case there was no way in which the leaks could be sealed up directly, short of rebuilding a major part of the rotation transmitting mechanism. To avoid this, an attempt was made to seal the leaks with an epoxy coating. A water-thin coating of Fuller's Resiweld<sup>(1)</sup> 7221 thinned 2:1 with SOV-3 thinner was applied to the atmospheric side of the bellows with

---

1. H. B. Fuller Company, St. Paul, Minnesota



a brush while the tube was evacuated and the coating was allowed to cure overnight. This treatment was completely successful in sealing the leaks permanently. No leak larger than  $10^{-13}$  liter-atmosphere/sec (the sensitivity limit of our Veeco MS-7 leak detector) remained, and the tube stayed vacuum tight after prolonged baking at  $250^{\circ}\text{C}$ . This temperature was regarded as the safe upper limit for baking out the epoxy coating; unfortunately such a temperature does not suffice for outgassing the tube very rapidly, and about two weeks of pumping with daily bakes for several hours at  $250^{\circ}\text{C}$  were needed to evacuate the tube to the  $10^{-9}$  torr region. The lowest pressure attained was  $2 \times 10^{-9}$  torr with the valve to the diffusion pump closed and a 1 liter/sec VacIon appendage pump in operation on the tube. The only getter used was a titanium-wrapped tungsten filament from which a little Ti was evaporated in a small attached ionization gauge. Molybdenum getters in the main tube (see 1st Quarterly Report) were outgassed but no Mo was evaporated in order to avoid any premature loss of tube wall light transmission.

The first quarterly report described an all glass, bakeable, ultra vacuum valve that was developed for this project. The valve uses indium as a sealing material and operation of the valve entails melting the indium and inserting a large diameter glass tube into it. The seal depends on molten indium wetting the glass and maintaining intimate contact when it solidifies. The conductance of this valve is high, and it has proven generally satisfactory through a number of tests. Occasionally, the surface of the glass tube that must be wet by indium to make a seal gets contaminated during bakeout, and a leaky seal results. While such a failure is infrequent, it was a cause for some concern. Fortunately, during the quarter a bakeable indium valve<sup>(2)</sup> having a more positive acting seal appeared on the market. This valve operates by forcing a modified knife-edge into an indium washer, but it differs from other

---

2. Kane Engineering Company, Palo Alto, California

metal-to-metal valves in that very little torque is needed to close it. Consequently, it is relatively light and need not be mounted in a heavy, rigid fashion. Moreover, it can undergo many closures before the knife edge goes clear through the indium washer, and should this happen, it is a simple matter to remelt the indium under vacuum to re-form the washer. Since the seal does not depend upon indium wetting any surface, it is not affected by anything driven out of the tube during bakeout. Finally, the configuration of the valve makes a simpler, more compact mounting possible giving needed additional clearance for the angular distribution apparatus in the bakeout furnace and in the Helmholtz coils. The new valve was installed at the close of the reporting period and we have not yet had time to test it thoroughly.

Experiments to measure the rate of deposition of molybdenum as a getter material from .015" dia. filaments revealed that thermal conduction to nickel support wires was sufficient to cause some evaporation of nickel. Since it is intended that Mo deposition in the angular distribution tube shall also serve to produce a uniform standard work function everywhere in the tube, vaporization of nickel with the Mo should be avoided. Substitution of .010" dia. molybdenum operated at  $2200^{\circ}\text{K}$  (5 amperes) satisfactorily removed this difficulty. It was found that the transmission of a clean glass surface 4 cm. from such a filament (a  $3\frac{1}{2}$ " length of wire wound into a  $\frac{1}{8}$ " dia. loose helix) was reduced by 10% in 24 minutes by Mo deposition. Rough estimates of the optical constants of Mo films (reliable values do not seem to have been published) indicate that at least  $20 \text{ \AA}$  thickness and quite likely more is required to reduce light transmission by 10%.

The necessity of our knowing fairly accurately the time required to deposit a monolayer to avoid premature darkening of the tube wall prompts us to continue to investigate the rate of deposition of Mo films on glass. A colorimetric chemical analytical method has been chosen which should be sensitive enough to measure the 90% transmission films we are dealing with. The method

was originally devised for biochemical assay work and required modification. This has been done, and an initial determination has been made on a 90% transmission film deposited on a 1" dia. Pyrex window. This determination, though only to be regarded as tentative yet, indicates that a much thicker layer (order of  $150 \text{ \AA}$ ) was deposited than the estimated optical constants suggest. Final results of this work will appear in the next quarterly report. A by-product of the work will be a good set of optical constants for thin Mo films on glass.

#### 1.2 Photocathodes

An initial attempt to make an S-9 photocathode in the Hall effect tube by the atomic beam cesiation method<sup>(3)</sup> failed because of insufficient cesium in the reservoir of the beam oven. Only a very low photosensitivity developed in this cathode even after prolonged cesiation, and the first color change indicating formation of the compound CsSb only appeared near the edge of the Sb deposit where the antimony layer thinned out. A second attempt to make a cathode in this tube also failed because a defining aperture in the antimony beam became misaligned with the result that the cesium beam did not land on the Sb deposit.

Initially S-9 and S-11 photocathodes are being deposited over a stannous chloride conductive coating on a Pyrex glass substrate. The use of Pyrex here is a matter of convenience until plates of Corning 7052 glass of suitable thickness can be obtained. Then cathodes will be made on this glass, again with the conductive coating since use of such coatings is fairly common in image tubes. It is not likely that any differences will be found that can be attributed to the substrate glass type since it is believed that the stannous chloride coating serves as a fairly effective buffer between glass and photosensitive layer; in any case the differences in composition between 7740(Pyrex) and 7052

---

3. R. E. Simon, A. H. Sommer, B. H. Vine, "Improved Uniformity of Photocathode Sensitivity" ASD report #ASD-TDR-62-619 (Nov. '62)  
LAS-SR-224-12

are not likely to result in appreciable differences in impurity concentration in the photocathodes. The situation is different with soft glass substrates such as Corning 0080 lime-soda glass. It is difficult to produce a good stannous chloride conductive coating on lime-soda glasses by the vapor method we ordinarily employ. When used as photocathode substrates without such a conductive coating, soft glasses release appreciable quantities of sodium and potassium from the glass into the newly forming photocathode under the action of hot cesium vapor, and these alkali metals enhance the sensitivity, especially in the red. When the cathode is cesiated by the beam method, it is probable that there is much less release of Na and K, especially if the substrate is not heated very much, and under these conditions one should get a cathode that more closely resembles those produced on Pyrex or 7052 glass. So far this latter statement is a conjecture since we do not know of any comparison of cathodes prepared on different substrates by the atomic beam method, but we plan to look into this matter as time permits during the coming quarter using the Hall effect tube to prepare and measure the photocathodes.

### 1.3 Hall Effect Tube

Several years ago Sakata<sup>(4)</sup> made a rather extensive investigation of the signs and densities of free carriers responsible for conduction in cesium antimony photocathodes using Hall effect, resistivity vs. temperature, and thermoelectric power to determine that in unoxidized  $\text{Cs}_3\text{Sb}$  surfaces (S-4 and S-9 photocathodes) the carriers are holes (p-type conduction) and the densities range from about  $10^{15} \text{ cm}^{-3}$  to about  $10^{17} \text{ cm}^{-3}$  and occasionally somewhat higher. It is most unfortunate that Sakata neglected to make any photoelectric measurements on his surfaces from which some correlation between carrier

---

4. Sakata, T., J. Phys. Soc. Japan 8, 125, 272 (1953) and 9, 1030 (1954).

concentration and photoemissive properties might have been made. The need for such a correlation becomes acutely apparent when one sets about developing a theory for the energy angular distribution from  $\text{Cs}_3\text{Sb}$  photosurfaces. We are therefore undertaking to remedy Sakata's omission by studying Hall effect, spectral sensitivity, and integrated energy distribution of various photosurfaces in a tube of relatively simple configuration and of a size that will fit into a magnet that we have which produces a conveniently large field (1000 gauss) in a suitably large region ( $\sim 3'' \times 3'' \times 3''$ ).

The general form of the tube is shown in Fig. 1. The photocathode is deposited over platinum electrodes on the inner cylinder using beam cesiation. Then the cylinder is rotated magnetically through  $90^\circ$  into the measuring position. Electrical contact with one of the two current leads is maintained through a Pt-Pt frictional contact in the lower bearing, and contact to the upper current lead is via a tungsten wire resting on a Pt slip ring on the upper spindle of the inner cylinder. Similar slip-ring contacts on the body of the inner cylinder complete connections to the Hall potential electrodes. The inside wall of the outer cylinder is conductively coated with stannous chloride, and it serves as collector for photoelectrons. Energy distribution is measured by retarding potentials applied between photocathode and the conductive wall of the outer cylinder. The geometry is very nearly planar, thus the distribution of the component of electron energy normal to the photosurface is what is measured in this arrangement and not the distribution in energy of the total emission. The difference is not important for the purposes of the experiment.

The simplicity and versatility of the Hall effect tube make it well suited as a practice tube for perfecting our techniques of making photocathodes. It is presently equipped with two sidearms containing atomic beam ovens; a third can easily be added for making multi-alkali cathodes. The arrangement of electrical contacts to the cathode make it possible for the resistivity of the cathode to be monitored while alkali metal is being added in the form of an

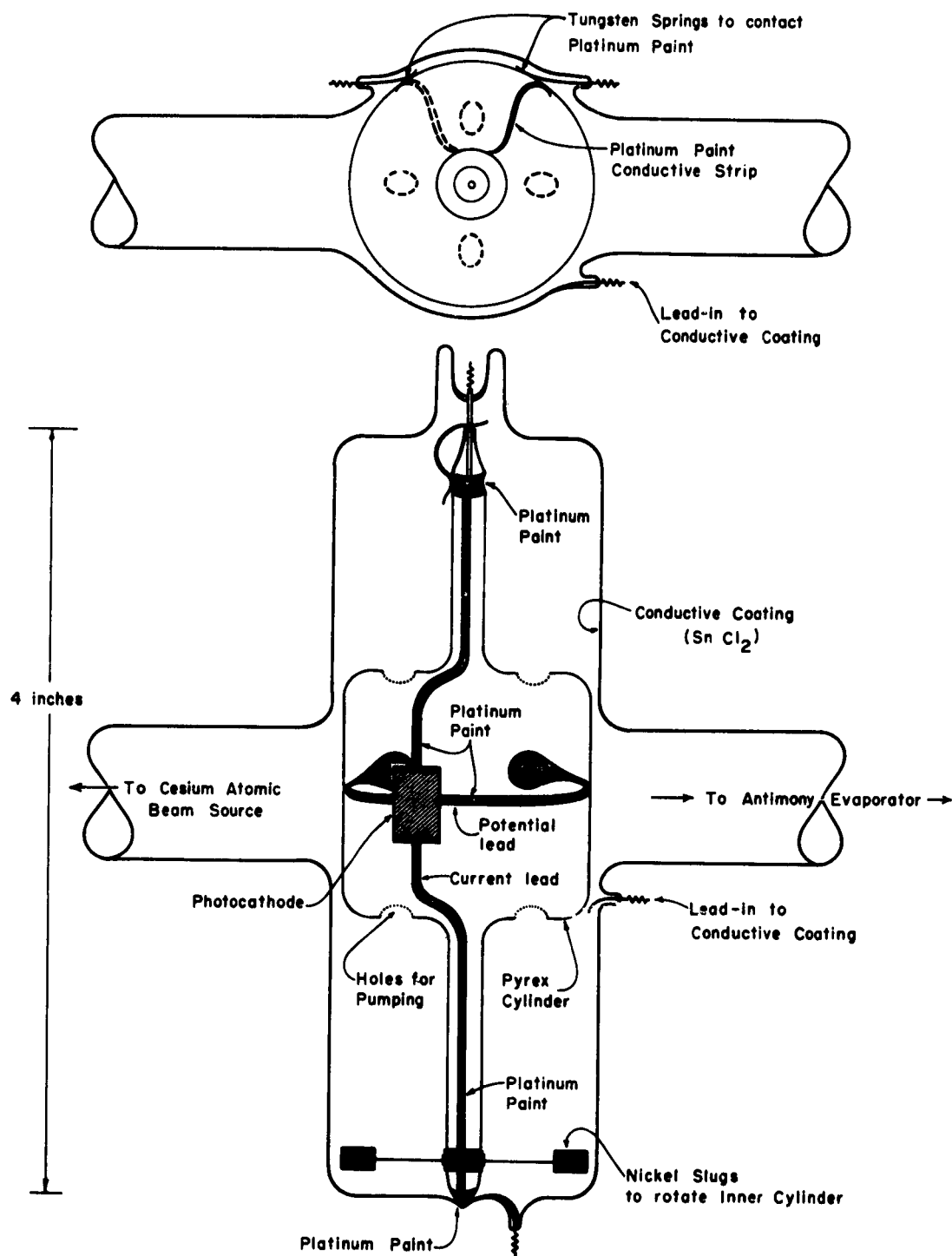


Figure 1. Hall effect phototube.

atomic beam, and this is expected to be a help in processing S-20 surfaces. The cylinder within a cylinder configuration is also helpful in keeping each alkali metal confined to its own sidearm during multialkali processing.

The Hall effect tube is normally pumped and baked out on a well baffled oil diffusion pump, gettered and sealed off, and subsequently pumped by an ionization gauge containing a titanium evaporator as described earlier. There has been no difficulty getting and maintaining a vacuum of  $10^{-9}$  torr with this arrangement even while cesiation is being carried on. It is of course necessary to degas the Sb and its evaporator thoroughly before seal-off and to degas the Cs pellets and finally to fire them before seal-off to get a good vacuum in the tube. The initial attempts at preparing S-9 cathodes mentioned earlier were all carried out in the Hall tube.

## 2. THEORETICAL

### 2.1 Introduction

During the reporting period we began a theoretical study of several aspects of the angular energy distribution of photoelectrons from  $\text{Cs}_3\text{Sb}$ . The work is still fragmentary as yet, but certain interesting features have already emerged, and we will give a brief account of these.

It is customary and convenient to divide the overall process of photoemission into four independent mechanisms:

Step 1. Penetration of the light wave into the surface layer of the photocathode. This in itself is a formidable problem to handle correctly. It is ordinarily treated by assuming the optical constants of the surface layer are independent of distance from the surface (which they are not) and applying classical electromagnetic theory to wave propagation in a homogeneous slab of material with constant refractive index and conductivity. The validity of this approximation does not seem to have been carefully examined, but it may be considerably in error. We shall discuss this question at length in a future

report in terms of a definite model of the surface conductivity of a semiconductor like  $\text{Cs}_3\text{Sb}$ .

Step 2. Optical excitation of electrons from the valence band of the semiconductor into the conduction band. This is ordinarily considered the least complex and best understood of the four processes we are discussing. However, it has much in common with step (1) above. For example, the optical absorption depends on conductivity which in turn depends on the optical excitation of valence electrons to the conduction band in semiconductors and insulators. Thus our steps (1) and (2) are not as independent as might appear at first. Furthermore, relatively few treatments of the primary photoabsorption process in the literature have taken properly into account the detailed properties of the solid particularly in regard to the effect of the lattice on the directions in which the excited electrons move initially away from the excitation site. More will be said about this point later.

Step 3. Motion of the excited electrons toward the surface. This is undoubtedly the least understood of our four processes involving as it does the extremely complex many-body interaction of the relatively energetic conduction electron with the other electrons and with the phonons of the solid. Behavior of conduction electrons in semiconductors near the bottom of the conduction band is fairly well understood, although a number of features of collective interactions of even these electrons is still relatively obscure particularly in polarizable solids. We are referring to the motion of slow polarons. But the behavior of fast polarons, the quasi-particles that we have principally to deal with in studying motion of internal photoelectrons with enough energy to escape, is an area of theoretical solid state physics that is virtually untouched. It is only within the past few years that attempts to deal with the polaron ground state have borne fruit.<sup>(5)</sup> Lacking any better guide we are forced to back to a fairly elementary

---

5. H. Fröhlich, *Advances in Physics* 3, 325 (1954).

G. R. Allcock, *Adv. in Physics* 5, 412 (1956).



approximate treatment of the fast polaron by Fröhlich and Mott <sup>(6)</sup> whose validity under conditions of interest here is admittedly very shaky.

Step 4. Escape of the photoelectron from the surface. This, too, is a process that has customarily received an uncritical treatment. The naïve picture of a free electron incident upon a step-potential barrier has been the basis of past treatments. Occasionally a slightly more realistic shape of potential barrier has been employed, but little has been attempted beyond this.

In view of the above criticisms why have the existing theories of photoemission been successful at all? The answer is that the theories are mainly phenomenological and contain enough adjustable parameters to allow reasonable agreement with experiment to be secured for many of the grosser photoelectric phenomena. This agreement does not necessarily mean that the simplified models of the individual processes involved in photoemission really describe what is taking place. More likely, the complexities of the actual mechanisms are somehow averaged out in the gross features of photoemission so they can be described by a much simpler model. This happens in secondary emission, for example, and it is common in many branches of physics leading to the result that one cannot deduce details of the mechanisms from experiments that measure averages. One must then either devise more sensitive experiments or attempt to construct more sophisticated models which still give the observed averaged properties but which also predict additional details that may eventually be tested.

These remarks are intended as a justification for taking a more critical view of photoelectric theories. Short of working with single crystal photoemitters, the present experimental program is designed to provide the

---

6. H. Fröhlich and N. F. Mott, Proc. Roy. Soc. A, 171, 496 (1939).

most detailed information possible about photoemission from semiconductors. It is to be expected that features will be found that are beyond the capabilities of present simplified theoretical models to account for. In anticipation of this, the initial objective in our theoretical work is to examine critically the weak points in present models and to see how these might be improved.

Three topics will be discussed briefly in this report: (1) the role of the lattice in the photoelectric absorption process that yields an excited conduction electron and a mobile hole, (2) the influence of the surface in the latter process, and finally (3) the mobility of an electron with escape velocity in a polar solid on the basis of the fast polaron theory of Fröhlich and Mott.

## 2.2 Photoelectric Absorption (Volume Effect)

The interaction of an optical photon with a lattice electron in the valence band of an infinite, regular solid may, as is well known, be treated by time-dependent perturbation theory which yields the probability

$$P_{12} = \frac{2\pi}{\hbar} |H_{12}|^2 \rho_2$$

per unit time for transitions from initial state 1 (electron in valence band and photon present) to state 2 (electron in conduction band, photon absorbed). The density of final states is here designated by  $\rho_2$  and the matrix element for the transition is  $H_{12}$  and has the following form in a perfect lattice of infinite extent,

$$H_{12} = \int U_{\underline{k}_2}^*(\underline{r}) e^{-i\underline{k}_2 \cdot \underline{r}} \left( -\frac{i\hbar e}{mc} \underline{A} \cdot \nabla \right) U_{\underline{k}_1}(\underline{r}) e^{i\underline{k}_1 \cdot \underline{r}} d^3 \underline{r} .$$

This is simply the interaction Hamiltonian between initial and final states of the electron which have been written in the form of simple Bloch wavefunctions,  $U_{\underline{k}}(\underline{r}) e^{i\underline{k} \cdot \underline{r}}$ , for brevity but which will generally consist of series of Bloch wavefunctions as required to satisfy the symmetry requirements of the lattice, the Kubic Harmonics of von der Lage and Bethe<sup>(7)</sup>. The interaction term, the

---

7. F. von der Lage and H. Bethe, Phys. Rev. 71, 612 (1947).

perturbation, is the  $\underline{A} \cdot \nabla$  term where  $\underline{A}$  is the vector potential of the light wave. For simple, undamped plane waves

$$\underline{A} = \underline{A}_0 e^{i(\omega t + \underline{k} \cdot \underline{r})}$$

where  $\underline{A}_0$  contains both amplitude and polarization and  $\underline{k}$  is the wavevector of the light wave. Of course, the proper  $\underline{A}$  to use is much less simple (see comments at the beginning of this section) but for present purposes the one given will serve.

The  $d^3\underline{r}$  integration variable contains the factor  $r^2 dr$  and  $\nabla$  contains a factor  $r^{-1}$  in spherical coordinates hence  $H_{12}$  is proportional to

$$\int e^{i(\underline{k}_1 - \underline{k}_2 + \underline{k}) \cdot \underline{r}} U_{\underline{k}_2}^* \underline{r} U_{\underline{k}_1} dr$$

and will vanish unless  $\underline{k}_2 = \underline{k}_1 + \underline{k} + \underline{n}$  where  $\underline{n}$  is a reciprocal lattice vector such that  $\underline{n} a/2\pi$  has integer components,  $a$  being the lattice spacing. If this quantity holds (conservation of momentum) there remains from the integral only the factor

$$\int U_{\underline{k}_2}^* \underline{r} U_{\underline{k}_1} dr$$

which will be recognized as the dipole matrix element for optical transitions between states 1 and 2 in the crystal.

The influence of the crystal field appears in two forms in the formulas above. First, the momentum conservation equation  $\underline{k}_2 = \underline{k}_1 + \underline{k} + \underline{n} \approx \underline{k}_1 + \underline{n}$  (because  $\underline{k}$  is very small for light waves of the wavelengths that we need consider) shows that optical excitation can be described by vertical (or nearly vertical) jumps in the reduced zone representation of energy  $E$  vs.  $\underline{k}$  for electrons of the crystal. This is important because, taken with the density of states function, it determines just where in momentum space the transitions are most likely to

occur, and this in turn tells a lot about the angular energy distribution. For certain common classes of crystals (and  $\text{Cs}_3\text{Sb}$  appears to be of this type), namely those having the minimum energy gap between valence and conduction bands located at  $\underline{k}_1 = 0$ , the momentum conservation equation reduces to

$$\underline{k}_2 = \underline{n}$$

which means that every newly photoexcited electron has its initial velocity directed along a principal direction  $\underline{n}$  in reciprocal space, hence along a principal direction in the actual lattice, provided  $\underline{n} \neq 0$ , a condition which always holds for interband transitions of the kind we are considering here.

A second way in which the lattice influences results is through the dipole matrix element,  $\int U_{\underline{k}_2}^* \underline{r} U_{\underline{k}_1} d\mathbf{r}$ . The kinds of terms permitted in the expansions for  $U_{\underline{k}}$  (i. e., in the Kubic Harmonics) are dictated by the symmetry properties of the crystal. As a result the matrix element actually consists of a series of terms, each consisting of an "allowed" type of dipole transition obeying selection rules quite analogous to those in optical spectra. Thus the selection rules govern the precise forms of the states that a given valence electron may reach via an optical transition. Note that both the final energy and momentum are already fixed by the conservation laws; the selection rules further delimit the possible transitions. Of these latter the relative strengths are governed by the magnitudes of the appropriate matrix element terms and by the density-of-states which require a quantitative knowledge of wavefunctions and band structure of excited states in the specific solid (here  $\text{Cs}_3\text{Sb}$ ) being studied. Solid state theory cannot provide either with any accuracy at present, but later in the course of this work we shall attempt some semiquantitative educated guesses about these things aided by our experimental results.

One interesting point should be mentioned before going on. We have showed that in  $\text{Cs}_3\text{Sb}$  the newly produced internal photoelectrons initially move

along major crystal axes so the angular distribution at the site of absorption of a primary photon is very sharply peaked. If an appreciable fraction of the excited electrons can move to the surface of the crystal without undergoing another strong collision which produces a large deflection it can be shown that the passage of the electron through the crystal surface into the vacuum outside may be treated to a first approximation as a refraction by the surface with predictable effects upon the internal angular distribution. The result is still a sharply peaked distribution outside the crystal for that part of the internal distribution that is peaked. In view of the long mean free paths for conduction electrons commonly believed to exist in  $\text{Cs}_3\text{Sb}$  ( $\geq 200 \text{ \AA}$ ), it would seem likely that many photoelectrons would indeed succeed in arriving at the surface essentially undeflected since they were initially excited. Therefore, if there is an appreciable degree of preferred crystallite orientation in a  $\text{Cs}_3\text{Sb}$  photocathode, the observed angular distribution should be more or less strongly peaked, the peaks being superimposed upon a cosine-like background. If no orientation exists and the crystallites are completely randomly oriented, then a simple cosine distribution would be expected even though a single crystal gives a highly peaked emission.

Thus far we have been treating the optical excitation of an electron in an infinite crystal. How does the proximity of a surface affect the results? That is, how does the excitation process differ in the surface and volume photo-effects? The answer must lie in the form of the electron wavefunctions that enter into the interaction matrix  $H_{12}$ . While we don't know a great deal about the detailed form of these wavefunctions, symmetry demands that they be strictly periodic in the surface plane, say the  $x, y$  plane, and almost periodic in the normal  $z$ -direction with a term added which depends only on the distance into the crystal and which in fact decreases as one goes into the crystal, vanishing at large distances  $z$  inside the crystal and leaving only the unperturbed volume wavefunctions. If we ignore the small variation in lattice spacing with  $z$  as

one approaches the surface it should be possible to construct a reasonably good wavefunction as follows: To the volume wavefunction  $\psi_{\underline{k}}(\underline{r})$ , which was explicitly written  $U_{\underline{k}}(\underline{r}) e^{i\underline{k} \cdot \underline{r}}$  earlier, we add a surface function,  $S_{\underline{k}}(z)$ , which decreases as  $e^{-a(\underline{k})z}$  for  $z > 0$  (i. e., as one goes into the crystal).

We allow for more general functions  $S(z)$  by using a series of the form

$\sum_{l=0}^{\infty} c_l e^{-a_l z}$  if necessary, but the simpler form will be sufficient for the present discussion. Finally, the resulting wavefunction,  $\Psi_{\underline{k}} = \psi_{\underline{k}}(\underline{r}) + S_{\underline{k}}(z)$ , is further defined to go to zero for all  $z < 0$  (outside the crystal) and this

may be enforced mathematically by multiplying the  $\Psi_{\underline{k}}$  written above by a unit step function which is unity for  $z > 0$  and zero for  $z < 0$ . The surface wavefunction  $S_{\underline{k}}(z)$  adds three new terms for the interaction matrix  $H_{12}$ .

One of these is a pure surface term of the form  $S_{\underline{k}_2}^*(z) V S_{\underline{k}_1}(z) d^3 \underline{r}$  where  $V$  stands for the  $\frac{-i\hbar e}{mc} \underline{A} \cdot \underline{\nabla}$  perturbation term. The remaining new terms in  $H_{12}$  involve mixed products of surface and volume wavefunctions such as  $\Psi_{\underline{k}_2} V S_{\underline{k}_1} d^3 \underline{r}$ . Consider the latter integrals first. They have the general form

$$\int_{\text{crystal space}} U_{\underline{k}_2}^*(\underline{r}) e^{-a_{\underline{k}_1} z} e^{-i\underline{k}_2 \cdot \underline{r}} d^3 \underline{r}$$

The exponential term is periodic in  $x$  and  $y$  but not in  $z$  except for large  $z \gg a_{\underline{k}_1}^{-1}$ . Thus near the surface momentum conservation in the  $x$   $y$  plane may be written  $\underline{k}_2 \times \underline{s} = \underline{n}_s$  where  $\underline{s}$  designates the surface normal unit vector and  $\underline{n}_s$  is a reciprocal vector of the surface lattice. Near the surface there is no longer the requirement that the  $z$ -component of  $\underline{k}_2$  be an integral multiple of a reciprocal

lattice vector. Both the presence of  $a_{\underline{k}_1} z$  in the exponential and the fact that the integrand vanishes for negative  $\underline{k}_1 z$  (outside the crystal) produce this change in behavior. Formally one may say that the  $z$  component of momentum is not conserved near the surface or that the surface as a whole supplies the deficit or takes up the excess. The pure surface integral contains an exponential of the form  $e^{-(a_{\underline{k}_1} + a_{\underline{k}_2})z}$ , and displays no conservation properties at all. This term is therefore in general not zero and makes some contribution to photoexcitation near the surface quite independent of the properties of the crystal except as they govern the distance  $a_{\underline{k}}^{-1}$  into the crystal through which the surface exerts its influence. This distance, it may be argued, is roughly equal to the Debye length,  $l_D = \left(\frac{\kappa k T}{4\pi N e^2}\right)^{1/2} = 6.7 \frac{\kappa T}{N} \text{ cm}$  where  $\kappa$  is the static dielectric constant,  $T$  is the absolute temperature, and  $N$  is the free carrier concentration in the solid. In  $\text{Cs}_3\text{Sb}$  at room temperature  $N$  ordinarily varies from  $\sim 10^{15} \text{ cm}^{-3}$  to  $10^{17} \text{ cm}^{-3}$  according to Sakata<sup>(4)</sup>, and optical measurements by Morgulis, Borziak, and Dyatlovitskaia<sup>(8)</sup>, gives values of the dielectric constant at long wavelengths as  $\sim 2$ . Thus the Debye length varies from about  $50 \text{ \AA}$  to  $500 \text{ \AA}$  depending on impurity concentration. Most of the evidence indicates that photoemission in  $\text{Cs}_3\text{Sb}$  comes from depths less than  $200\text{--}250 \text{ \AA}$  below the surface so it is evident that in very pure  $\text{Cs}_3\text{Sb}$  we have a predominantly surface photoeffect to consider while in cathodes with higher excess carrier concentrations ( $N \sim 10^{17} \text{ cm}^{-3}$ ) the surface contribution is small, and we are dealing mainly with a volume photoeffect. This is a very interesting situation for it gives us a favorable opportunity to study experimentally surface and volume photoemission in the same material

---

8. N. D. Morgulis, P. G. Borziak, and B. I. Dyatlovitskaia, *Izvest. Nauk. SSSR*, 12, 126 (1948).

at wavelengths that are conveniently reached. It has commonly been considered that the volume photoeffect can be studied only in the vacuum ultraviolet which is largely true for metals but not necessarily for semiconductors, as we have seen. An experimental investigation of the surface vs. volume photoeffect will be carried out in the Hall effect tube, described earlier, where the free carrier concentration (hence the Debye length) can be determined. As usual, it will be difficult to separate effects characteristic of the primary excitation process from those produced during transport of the excited electron to the surface and theory, such as it is, must be relied on to help in this.

Summing up what has been said about the primary excitation process in  $\text{Cs}_3\text{Sb}$ , we have shown that the volume photoeffect is characterized by vertical transitions in the reduced Brillouin zone scheme and that conservation of electron and lattice momentum cause excited electrons to have their initial velocities directed along principal crystal axes. In the surface effect, however, momentum conservation analogous to that in the volume effect takes place only in directions parallel to the surface. Normal to the surface a different and less restrictive condition applies. In both cases energy and momentum conservation supply two sets of selection rules for the transition. A third set is furnished by analogs of the usual selection rules for optical dipole transitions ( $\Delta L = \pm 1$ ,  $\Delta J = 0, \pm 1$ , etc.) which determine the exact crystal states between which transitions can take place. To carry the theory any further quantitatively, detailed electron wavefunctions are needed which are not available for  $\text{Cs}_3\text{Sb}$ . The theory can be further extended in a qualitative and perhaps in a semiquantitative way through group theoretic arguments, and this will be done in the near future.

Turning finally to the problem of electron transport to the surface, it has already been pointed out that this involves the dynamics of a fast polaron. A polaron is a quasi-particle which is the aggregate of a conduction electron and its surrounding polarization cloud representing the polarizing effect of the Coulomb field of the electron on its surroundings. The result of polarization induced by



the electron is to shield out the Coulomb field, converting the Coulomb potential  $e^2/\kappa r$  into the shielded Coulomb potential  $\frac{e^2}{\kappa r} e^{-r/l}$  where  $l$  is the shielding length and is at least comparable, if not identical, with the Debye length when the electron is static or moving very slowly. For faster electrons, and these include electrons with enough energy to escape the surface barrier in  $\text{Cs}_3\text{Sb}$ , the polarization cannot develop and decay rapidly enough as the electron passes by a given region of the lattice for the full shielding effect to become established. Parts of the lattice relatively far from the electron path do have time to respond. If the distance of closest approach of the electron to the lattice atom under consideration is  $b$  and the electron velocity is  $v$ , then the "collision time" is of the order  $b/v$ , and the atom can be fully polarized for  $b/v$  greater than the orbital velocity of its outer shell electrons (i. e., those remaining after the atom has contributed its share to the valence band of the solid. The orbital periods of these electrons which are ordinarily bound with the order of some tens of electron volts of energy are approximately  $\hbar/E$ , or order of  $2 \times 10^{-16}$  seconds and the conduction electrons with escape velocity move with  $v \approx 10^3$  cm/sec. Therefore atoms closer to the electron path than a few angstroms are not fully polarized and do not contribute fully to the shielding. As a result the shielding length is larger for fast electrons and these electrons can therefore collide with other charged particles in the solid over a greater range than slower electrons. We see by this simple argument that the character of the charge distribution is different for fast and slow polarons and their collision cross sections are also different. The fast polaron has a larger cross section for inelastic, energy-dissipating collisions with other charged particles in the lattice but not necessarily an appreciably different cross section than the slow or static polaron for energy losses via collisions with lattice phonons. The polaron-phonon cross section depends mainly upon the gross size of the polaron, chiefly upon the overall extent of the polarization cloud while the polaron-charged particle cross section depends more upon the detailed charge distribution, particularly upon the size of the relatively unshielded core of the polaron which, as we have shown, increases with velocity.

The simple qualitative model of a fast polaron outlined above permits some general conclusions about the rate of energy loss by such a particle and about its mean free path. The energy loss rate of an electron interacting via an unscreened Coulomb potential with a collection of charged particles is proportional to  $E^{-1} \left( \frac{b_{\max}}{b_{\min}} \right)$  by the well-known Bohr collision theory<sup>(9)</sup> where  $b_{\max}$  and  $b_{\min}$  are suitable cutoff values of the closest approach distance chosen (by arguments that we need not go into here) to insure convergence of the final result. The important point for this discussion is that for the polaron  $b_{\max}$  is essentially the size of the polaron since shielding causes its interaction with charged particles beyond the shielding length  $l$  to fall off rapidly. Fast polarons have larger  $l$ , as we have seen, and therefore they have larger values of  $b_{\max}$  than slow polarons and consequently suffer a slightly higher rate of energy loss. It follows also that fast polarons have slightly shorter mean free paths. The difference is small because of the logarithmic dependence on  $b_{\max}$ . These conclusions apply to collisions of polarons with other charged particles in the lattice considered individually. Regarding collisions with phonons the situation is not so simple. The polarization surrounding a conduction electron may be thought of as a cloud of transverse or optical phonons.<sup>(10)</sup> This cloud is stationary if the electron is at rest and may then be described by a superposition of transverse phonon waves of appropriate wavelengths chosen in such a way as to give a stationary distribution of polarization. The phonon wavelengths needed to describe the polaron range downward from a maximum  $\lambda \approx 2 l$  where  $l$  is as before the "size" of the polaron to a minimum of the order of the shortest transverse phonon wave-

---

9. N. Bohr, Phil. Mag. 24, 10 (1913), 30, 581 (1915).

10. H. Fröhlich, Proc. Roy. Soc. (London) Ser. A, 160, 230 (1937).

length that can propagate through the crystal. Now the polaron can interact strongly only with those transvers. phonons in the crystal having wavelengths comparable with wavelengths of the phonons making up the polarization cloud of the polaron. The interaction therefore depends on the density of optical phonons that normally exist in the right range of wavelengths in the crystal. The Debye temperature  $\theta_D$ , is an approximate measure of the energy of the shortest wavelength phonons in a crystal. Actually, the Einstein temperature,  $\theta_E$ , measures this quantity for optical phonons but when the masses of the two ions are nearly the same, as in  $\text{Cs}_3\text{Sb}$ , the Debye and Einstein temperatures are also nearly the same. Unfortunately neither  $\theta_D$  nor  $\theta_E$  is known reliably for  $\text{Cs}_3\text{Sb}$ .  $\theta_E$  is probably the order of 50-100°K judging from values for other weakly bound valence-bonded compounds having large heavy atoms. Additional evidence for a low Debye temperature comes from the fact that the photo-emission of  $\text{Cs}_3\text{Sb}$  begins to fall off at liquid nitrogen temperatures and below<sup>(11)</sup> which we interpret as due to a deficiency of high energy phonons required for conservation of momentum in the primary excitation process. This is a point that will be discussed quantitatively in a future report. Finally, X-ray analysis by Jack and Wachtel<sup>(12)</sup> e  $\theta_D = 59^\circ\text{K}$  for the Cs atoms and  $\theta_D = 131^\circ\text{K}$  for the Sb atoms in  $\text{Cs}_3\text{Sb}$ , the average value being  $85^\circ\text{K}$ . If we take  $\theta_E = \frac{3}{4}\theta_D = 65^\circ\text{K}$ , which is accurate enough for the present discussion, the highest frequency transverse phonon has a frequency of  $1.3 \times 10^{12} \text{ sec}^{-1}$  and a propagation velocity  $C_t \approx 1.4 \times 10^5 \text{ cm/sec}$ . This latter comes from an approximation used in the Debye theory of specific heats which relates  $\theta_D$  to a certain function of the transverse and longitudinal sound velocities. These are in turn connected in a well-

---

11. A. T. Young, *Applied Optics* 2, 51 (1963).

12. K. H. Jack and M. M. Wachtel, *Proc. Roy. Soc. A*, 239, 46 (1957).

known way by an expression involving the Poisson ratio  $\sigma$  of the substance which lacking any better basis, we have taken as  $\frac{1}{4}$ , a value typical of many materials. With these approximations and the resulting transverse velocity,  $C_t$ , we arrive at a maximum value for the transverse wavenumber,  $k_{\max} = \frac{1}{\lambda_{\min}} = \frac{vE}{C_t} \approx 6 \times 10^7 \text{ cm}^{-1}$ . The value of  $k$  at the zone boundary in  $\text{Cs}_3\text{Sb}$  is about  $3.4 \times 10^7 \text{ cm}^{-1}$  based on Jack and Wachtel's value  $9.15 \text{ \AA}^0$  for the size of the unit cell. Comparison of these two figures shows that in  $\text{Cs}_3\text{Sb}$  only relatively long wavelength transverse phonons (small  $k$ ) are present. Moreover, the shortest wavelengths present in the crystal ( $k_{\max}^{-1}$  or  $\sim 18 \text{ \AA}^0$ ) are much longer than those making up the fast polarons ( $\lambda \lesssim 4 \text{ \AA}^0$ ). Therefore, we conclude on the basis of this simple model of the fast polaron that the polarons do not interact strongly with the lattice phonons, that the photoemission should not be appreciably temperature dependent at ordinary temperatures, and that the mobility and energy loss rate of the polaron should not vary appreciably with polaron energy since at energies of interest here the polaron never spreads out enough to allow it to interact with the lattice phonons. The lattice and polaron phonons simply occupy different regions of  $k$ -space and these regions do not overlap sufficiently to allow much interaction. The principal scattering agent for conduction electrons with escape velocities  $\text{Cs}_3\text{Sb}$  must therefore be something other than lattice vibrations. Impurities and excitons are likely possibilities to be explored. Also in view of the implications of the simple analysis given above we plan to refine the arguments more quantitatively for a future report.